TECHNOLOGIES AND ENGINEERING

Journal homepage: https://technologies-engineering.com.ua/en
Vol. 26, No. 3, 2025

Received: 03.02.2025
Revised: 21.05.2025
Accepted: 25.06.2025

UDC 621.372.8:004.7

DOI: 10.30857/2786-5371.2025.3.1

Ultra-wideband transmission lines for next-generation digital systems: Modelling and analysis

Serhii Boichenko*

Postgraduate Student
Kharkiv National University of Radio Electronics
61000, 14 Nauky Ave., Kharkiv, Ukraine
https://orcid.org/0009-0008-6118-8314

Abstract. The study aimed to theoretically analyse the modelling of pulse transmission in ultra-wide bandwidth media with consideration of losses, dispersion and phase shifts. A comprehensive approach was used, combining mathematical modelling and analysis of electromagnetic processes in various transmission line topologies, such as coaxial, stripline, microstrip, and structures based on metamaterials and superconductors. The study determined that the dispersion, frequency-dependent losses caused by the surface resistance, which increased proportionally to the root of the frequency, and dielectric losses with a frequency-dependent tangent caused distortion of pulses with delays of 10-100 picoseconds and phase shifts of up to 20 degrees. For pulses with a duration of 0.5 nanoseconds, the spectral width was about 2 GHz, which confirmed the dependence between the pulse duration and the frequency range. Modelling using the telegraphic equations, the Fourier transform and numerical methods such as finite difference time domain and finite element analysis quantified losses of up to 3-6 decibels per 10 cm and the critical line length, which depended on geometric inhomogeneities. The advantages of superconducting structures with losses of less than 0.01 decibels per metre up to 100 GHz and coplanar lines for transmission speeds of 25-50 Gbps were revealed. The frequency-dependent performance criteria were formulated for a reasonable choice of the line type depending on the requirements for minimising phase shifts and pulse attenuation. The practical significance of the results is determined by the possibility of their use by specialists in the design of telecommunications and sensor systems to improve the reliability and accuracy of data transmission in real-world conditions

Keywords: dispersion; surface resistance; pulse signal; frequency-dependent losses; metamaterials; superconductors; phase stability

Introduction

The development of digital technologies in the 21st century, including 5G and 6G communication systems, high-speed networks, and an increase in the amount of data transmitted, necessitates fundamentally new solutions in the field of signal transmission lines. One of the most promising areas is Ultra-Wideband Transmission Line (UWB-TL), which provides high bandwidth, low power consumption and the ability to operate in conditions of strong spectral noise. Their implementation is important for applications such as wireless power transmission, ultrafast data communications, microwave photonics, high-precision positioning systems and edge computing. In the scientific literature, there is an increasing interest in research on modelling UWB systems. They focus on solutions that can adapt to changing environmental conditions and minimise losses. At the level of system architecture, attention is focused on the impact of antenna configuration and combining networks on the efficiency of power transmission.

In the context of a wide frequency range, it is worth citing the study by S. Roy *et al.* (2023), which demonstrated that phased array antennas provide higher resistance to spectral interference compared to traditional combining networks, indicating their suitability for conditions with variable radio-frequency (RF) characteristics. The obtained results demonstrated the relevance of using UWB components in environments with a high level of RF disturbances.

Suggested Citation:

Boichenko, S. (2025). Ultra-wideband transmission lines for next-generation digital systems: Modelling and analysis. *Technologies and Engineering,* 26(3), 11-23. doi: 10.30857/2786-5371.2025.3.1.

*Corresponding author

A separate area is the miniaturisation of components while maintaining effective alignment. The study by S.-Z. Liu *et al.* (2025) presented a ferrite circulator optimised for UWB operation. The authors showed that the appropriate selection of materials and geometric parameters can achieve compactness while maintaining key performance characteristics, which is important for the integration of such components into multifunctional digital platforms. Improving the efficiency of impedance matching in UWB structures is also associated with the development of compact filters capable of operating in a wide frequency range with high selectivity. A. Kayalvizhi *et al.* (2025) considered the design of a bandpass filter based on an open loop with a discontinuity intended for use in wireless devices. Numerical modelling and verification of the layout were conducted to establish the stability of transmission characteristics in the ultra-wideband mode, with effective impedance matching and low losses within a given frequency band. The proposed circuitry solution provided the necessary conditions for the functioning of components in digital systems operating in a wide frequency range.

The development of switching structures has formed a separate branch of research. A. Fisher *et al.* (2025) demonstrated the potential of using silicon plasma as an active element of an ultrafast switch with low losses. This approach has opened new perspectives for building adaptive paths in UWB systems, where switching time and stability of signal parameters are of key importance. Regarding physical transitions between line types, for example, from coplanar to microstrip, the study by G.H. Lee *et al.* (2021) is notable. The study proposed compact transitions from coplanar lines to microstrip lines using a curved structure on a two-layer substrate. These transitions provide high efficiency in a wide frequency range from 2 to 17 GHz and minimal transition losses of up to 2 dB. Good performance has been demonstrated, making them useful for high-density microelectronic component applications where compactness and precise parameter matching are important. This confirmed the importance of developing efficient solutions for UWB links in high-speed digital paths. Digital distortion compensation is another critical area that is also gaining importance. The deep Sequence-to-Sequence neural architectures for modelling fibre-optic media presented by M. Shi *et al.* (2025) have a high level of dispersion and nonlinearities. Despite the different physical nature of the systems, their analytical principles and results demonstrate high relevance to UWB environments. The study proved that digital signal processing based on artificial intelligence can significantly improve transmission accuracy even in difficult conditions.

Ukraine is also developing ultra-wideband technologies in applied and fundamental research, in particular, the development and improvement of antennas, transmission lines and pulsed UWB systems. The modelling and analysis of broadband transceiver structures is also being addressed with increasing intensity. D.O. Batrakov *et al.* (2024) proposed a system for detecting subsurface cracks in non-rigid pavement using ultra-wideband GPR. The use of two receiving antennas with orthogonal polarisation made it possible to record cross-polarisation components of the signal. Experimental studies conducted on motorways in Ukraine have confirmed the effectiveness of the approach in a complex environment. The work is an example of the use of UWB transmission lines in a complex heterogeneous environment, which is of high practical importance.

Additionally, F.F. Dubrovka *et al.* (2023) presented the development of an ultra-compact biconical antenna for unmanned aerial vehicles with support for various types of polarisations (circular, horizontal, vertical and tilted). The antenna was modelled, fabricated and measured in the range of 2-18 GHz. The revealed effect of multiple resonant reflections was used to analyse the influence of geometry on the voltage standing wave ratio and gain, which is important for the development of UWB technologies in avionics. Pulsed UWB signals received by a ferrite antenna with a two-turn helix were analysed in the time and energy domains using Finite-Difference Time-Domain (FDTD) modelling in T. Ogurtsova *et al.* (2023). The results showed the dependence of the signal characteristics on the load and geometry, which highlighted the theoretical aspects of modelling UWB lines in receiving systems.

Despite a significant number of theoretical and applied developments in UWB-TL modelling, an integrated approach to considering electromagnetic, thermal and nonlinear effects used in chips and adapting numerical methods (moments, FDTD) for the complex geometry of ultrawideband structures remains insufficiently developed. Therefore, the study aimed to theoretically substantiate the principles of modelling and analysing the processes of pulse signal transmission in ultra-wideband lines to ensure their efficiency in digital systems, considering dispersion, frequency-dependent losses and phase stability. To achieve this goal, the following objectives were set: to systematise the physical mechanisms of pulse signal distortion in UWB-TL, to analyse mathematical models of UWB signal transmission lines, to conduct a comparative analysis of typical transmission line configurations, and to formulate recommendations for selecting and optimising UWB lines for phase stability and loss minimisation.

Materials and Methods

The study involved a theoretical modelling and analysis of the processes of pulse signal transmission via UWB-TL, combining theoretical, numerical and analytical methods for modelling dispersion, losses and nonlinear effects in UWB transmission lines. The choice of methods was based on their ability to reflect the diverse line structures and practical applications in 21st-century technologies. Seven types of UWB transmission lines were selected for analysis: coaxial, stripline, microstrip, Coplanar Stripline (CPS), Coplanar Waveguide (CPW), metamaterial and superconducting structures. Their choice was based on a wide range of technical characteristics and application scenarios in broadband transmission technologies. The selected configurations are discussed in terms of their electromagnetic properties, limitations, and typical applications.

In addition, standardised numerical modelling methods and mathematical models were used to analyse and evaluate the behaviour of transmission lines under real operational loads. To quantitatively described electromagnetic processes, the RLGC-line model (a generalised representation of the distributed longitudinal distributed parameters of a transmission line that describes electromagnetic processes in telegraphic equations) was used. It is characterised by four parameters per unit length: R – ohmic resistance of conductors, which takes into account conduction losses, in particular the surface effect in the UWB mode, L – inductance, which models the accumulation of magnetic field energy around conductors, G – conductivity between conductors, which describes losses in the dielectric, C – capacitance between conductors, which determines the accumulation of electric field energy), which described transmission lines as a linear system with distributed parameters (1, 2):

$$\frac{\partial V(x,t)}{\partial x} = -L\frac{\partial I(x,t)}{\partial t} - RI(x,t), \quad (1)$$

$$\frac{\partial I(x,t)}{\partial x} = -C\frac{\partial V(x,t)}{\partial t} - GV(x,t), \quad (2)$$

where V(x,t) – voltage at point x at time t; I(x,t) – current at point x at time t. These equations define the transmission function of a transmission line as a function of frequency H(f), incorporating $Z_0(f)$ and α(f).

The losses in conductive materials during signal propagation were described through the surface resistance, which depends on the frequency (3):

$$R_s(f) = \sqrt{\frac{\pi f \mu_0 \rho}{2}}, \quad (3)$$

where f – frequency of the electromagnetic signal; – magnetic permeability of the vacuum (physical constant established by the International System of Units $4\pi \times 10^{-7}$.

Any pulse signal x(t) can be represented as a direct Fourier transform (4) (Oppenheim *et al.*, 1997):

$$X(f) = \int_{-\infty}^{\infty} x(t)e^{-j2\pi ft}dt, \quad (4)$$

where X(f) – complex spectral amplitude of the signal at frequency f determines the frequency component of the signal x(t) in the form of a complex number containing both amplitude and phase information; $\int_{-\infty}^{\infty}$ – an integral over the entire time domain, which provides full coverage of the signal (this means that the analysis was performed considering all time points from minus to plus infinity); $e^{-j2\pi ft}$ – the original signal in the time domain that is subject to spectral analysis (this is a real- or complex-time function that describes the signal amplitude at each time point t, dt – a complex exponent that acts as the base transformation function. In this case, $e^{-j2\pi ft}$ – an analyser function that "extracts" the frequency component f from the signal x(t), j – imaginary unit (j^2=-1 is used in engineering instead of i to avoid confusion with electric current), 2πft – phase shift that depends on time and frequency, dt – differential of the integration variable t, indicating that integration was performed on the time variable.

Given a known frequency response of the transmission line H(f), the spectrum of the signal after passing through the line is (5):

$$Y(f) = H(f) \cdot X(f). \quad (5)$$

This corresponds to the convolution of the signal with the impulse response of the line in the time domain. The inverse Fourier transform restores the signal in the time domain (6):

$$y(t) = \int_{-\infty}^{\infty} Y(f)e^{j2\pi ft}df, \quad (6)$$

where y(t) – restored signal in the time domain; Y(f) – spectral function obtained as a result of the direct Fourier transform; df – frequency differential that defines the integration variable in the spectral domain.

In applied engineering problems, the analytical Fourier transform is implemented in a discrete form. For this purpose, a discrete Fourier transform is used, which grounds calculations based on a finite number of signal samples (7):

$$X[k] = \sum_{n=0}^{N-1} x[n] \cdot e^{-j\frac{2\pi kn}{N}}, \quad (7)$$

where X[k] – complex spectral value at the kth harmonic; x[n] – signal value in the time domain at the nth discrete step; $e^{-j\frac{2\pi kn}{N}}$ – basic exponential function corresponding to the kkkth harmonic; k – frequency index (from 0 to N-1); N – total number of points or samples (signal length). This transformation converts the signal from the time domain to the frequency domain, where each X[k] represents the amplitude and phase of the corresponding frequency component.

The inverse Fourier transform (8) (Küpfmüller, 1928) is used to recover the signal from its spectrum:

$$x[n] = \frac{1}{N}\sum_{k=)}^{N-1} X[k] \cdot e^{-j\frac{2\pi kn}{N}}, \quad (8)$$

where x[n] – restored signal value in the time domain at a discrete step nnn; $\frac{1}{N}$ – normalisation factor that ensures the preservation of signal energy when moving from the frequency domain back to the time domain.

Based on the literature data by M.-J. Kim *et al*. (2024), B.-C. Min *et al*. (2024) and Y. Weng *et al*. (2025) summarised UWB-TL modelling methods by their implementation and examples of application in real systems. To analyse the behaviour of UWB transmission lines in real conditions, numerical methods, such as FDTD and finite element method (FEM), system identification methods were considered to more accurately assess the behaviour of lines in real conditions. This approach optimised the UWB-TL parameters to minimise losses and distortion in a wide frequency range. Additionally, the parameters that affect the distortion of pulse signals in UWB transmission lines were investigated: time delay of the edge, maximum

amplitude offset, integrated loss energy, optimisation of transmission line design, loss and distortion analysis, and sensitivity to transmission line topology. The parameters were evaluated concerning real-world conditions and applied to numerical models to analyse and optimise transmission line performance, ensuring minimal pulse distortion in UWB systems.

The types of UWB transmission lines and their applications in electronic systems of the Internet of Things (IoT) and Wireless Body Area Network (WBAN), ultrafast digital interfaces, 5G/6G systems, superconducting and MicroElectroMechanical Systems (MEMS) technologies, sensitivity to geometry and operating conditions are analysed to describe in detail the technical parameters of UWB-TL, assess their effectiveness in real applications and compare different transmission line designs for applications in various electronic and telecommunication systems. The choice of UWB transmission line types was made based on their ability to meet the specific requirements of different systems: for IoT and WBAN, accuracy and resistance to fluctuations are important, for 5G/6G, transmission speed and low losses, for superconducting technologies, minimal losses and phase stability. Based on the analysis of the results, practical recommendations were formulated for the further development of UWB-TL technologies.

The Zotero bibliographic manager was used to process the literature sources, which ensured the systematisation of scientific publications and their thematic classification. For the theoretical analysis of the electromagnetic characteristics of UWB-TL, the Ansys High-Frequency Structure Simulator (HFSS) software was used to assess the influence of frequency-dependent parameters and geometric characteristics on the behaviour of signals in various UWB-TL structures. Ansys HFSS was chosen because of its ability to accurately simulate electromagnetic processes in broadband systems, which estimated the frequency-dependent loss, dispersion, and phase stability of UWB-TL.

Results and Discussion

The term UWB-TL refers to structures that provide stable electromagnetic signal transmission over a wide frequency range. UWB systems cover a frequency band of more than 500 MHz or at least 20% of the centre frequency. In the context of transmission lines, this means the ability to provide a uniform transmission characteristic (in particular, in phase and amplitude) over the frequency range required to transmit pulses on a nanosecond or picosecond scale. Such structures include coaxial, strip, microstrip, and metamaterial-based topologies and MEMS technologies. UWB-TLs are widely used in digital signal processing systems, wireless data transmission, pulse radar, and IoT devices (Kim *et al.*, 2024). A classical digital pulse is a time-limited signal containing a set of harmonic components in its spectral structure. According to the Fourier uncertainty principle, the shorter the pulse in the time domain, the wider the spectrum of its frequency representation (Küpfmüller, 1928). This is quantitatively expressed as (9):

$$\Delta f \geq \frac{1}{t}, \quad (9)$$

where Δf – spectrum width (working frequency band); t – spectrum width (working frequency band); effective pulse duration.

For pulses with a duration of 0.5 ns, a frequency band of approximately 2 GHz is typical. In such conditions, traditional transmission lines become unsuitable due to increased losses, dispersion and nonlinear effects. In broadband conductive media, the electromagnetic wave undergoes significant deformation due to dispersion and loss effects. Dispersion causes different phase and group velocities for individual spectral components of the signal, which leads to a distortion of its time form. Frequency-dependent losses, mainly caused by an increase in the surface resistance of conductors $R_s \sim \sqrt{f}$ and dielectric losses in insulating materials, further degrade signal integrity. Spatial inhomogeneities in the medium cause partial reflections and variations in group delay, which also affect the quality of pulse transmission. Even with a relatively short transmission line length (10-20 cm), a picosecond pulse is subject to significant distortion (Oppenheim *et al.*, 1997). Therefore, modelling such distortions and taking them into account at the design stage is critical to ensure reliable transmission of ultra-wideband signals. Transmission of pulses with an ultra-wide spectrum requires the use of transmission line structures that provide minimal losses, stable phase and amplitude response over a wide frequency range. Classical solutions include coaxial, stripline, and planar lines, but modern technologies also use metamaterial and superconducting approaches (Table 1).

Table 1. *Classification of transmission lines by the principle of implementation and area of use*

Structure type	Characteristics and features	Application examples
Coaxial lines	Symmetrical design with a central conductor and shield to minimise electromagnetic radiation and sensitivity to external disturbances. Provide stable wave impedance ($Z_0(f)$) in the range up to 20-30 GHz due to the choice of dielectric (e.g., silicon substrates) and precise conductor design. Limitations: high production costs for ultra-high frequencies.	MEMS-based coaxial line array for IoT devices with broadband signal transmission.
Strip lines	A planar structure with a conductor between two grounded layers, which enables high integration with digital and RF components. Supports frequencies up to 10 GHz and above, but is sensitive to dielectric substrate inhomogeneities that cause phase distortion and loss.	Vertical junctions in stripline structures for ultra-high-speed digital interfaces.
Microstrip lines	Conductor on a dielectric substrate with a ground at the bottom for easy manufacturing and compatibility with multilayer boards. Sensitive to dielectric losses and surface resistance ($R_s \sim \sqrt{f}$), which limits their effectiveness at frequencies above 15 GHz.	Filters with defective ground structure for mm-waves in multilayer boards.

Table 1. Continued

Structure type	Characteristics and features	Application examples
CPS	Two parallel conductors on a single dielectric layer, providing high integration with planar circuits and low losses at frequencies up to 10 GHz. Supports autonomous phase balancing, but requires precise geometry control to minimise parasitic effects.	CPS structures in data transmission systems with autonomous phase balancing.
CPW	A central conductor with grounded planes on each side on a single layer, combining the advantages of microstripes (simplicity) and symmetrical lines (broadband). Provides effective adaptation to planar antennas at frequencies up to 20 GHz, but is sensitive to substrate inhomogeneities.	UWB antennas for high-bandwidth wireless networks.
Metamaterials	Structures with non-standard electromagnetic properties (e.g. negative dielectric constant) that enable miniaturisation and bandwidth expansion up to 30 GHz and beyond. Require complex design and precision manufacturing.	Metasurface UWB antennas for WBAN with improved gain and bandwidth.
Superconducting structures	Superconducting materials are used to reduce surface resistance $R_s(f)$, providing almost zero losses up to 100 GHz. Provide high efficiency but require cryogenic cooling, which complicates practical application.	Magic-T structure for mm/submm cameras in the 6-14 GHz range, pulsed sensor systems and quantum electronics.

Source: *compiled by the author based on M.-J. Kim et al. (2024), B.-C. Min et al. (2024), Y. Zhu et al. (2024), S. Inoue et al. (2024), Y. Weng et al. (2025), X. Li et al. (2025)*

UWB-TL is represented by a variety of structures, each of which has specific characteristics that determine its application in high-speed systems. Coaxial lines provide stability and minimal loss at high frequencies but are expensive to manufacture. Planar structures, such as stripline, microstrip, CPS and CPW, are easy to integrate with digital and RF components, but their performance is limited by their sensitivity to inhomogeneities and dielectric losses. Metamaterials open opportunities for miniaturisation and bandwidth expansion, while superconducting structures provide minimal losses in the millimetre range but require sophisticated cryogenic support. Superconducting materials can significantly reduce the surface resistance, which, accordingly, minimises power losses during the propagation of high-frequency pulses. In such structures, the impedance becomes complex (10):

$$Z_s(f) = R_s(f) + jX_s(f), \quad (10)$$

where $R_s(f)$ – frequency-dependent active (ohmic) resistance, which is mainly due to the surface current effect (surface effect); $X_s(f)$ – the reactive component, which describes the inductive properties of the surface layer. The choice of a specific structure depends on frequency range requirements, technological integration, and economic feasibility, which underlines the importance of further research to optimise UWB-TL in modern telecommunications systems. For the quantitative description and modelling of broadband transmission lines, the following frequency-dependent functions are used as the basis for modelling pulse distortion. $Z_O(f)$ – wave (characteristic) impedance; $\alpha(f)$ – attenuation coefficient, including losses in the conductor and dielectric; $\beta(f)$ – phase constant (rad/m) associated with group delay; $R_s(f)$ – surface resistance of the conductor, which increases with frequency as $\sqrt{f}$.

Effective UWB-TL design requires the use of mathematical models capable of adequately describing both the frequency and time behaviour of signals during their propagation in an electromagnetic medium. The main task of such modelling is to quantify the changes in the pulse signal caused by the combined effect of losses, dispersion phenomena and distortions caused by the geometry of the conductive structure, electrophysical properties of materials, as well as boundary conditions that form the configuration of the transmission line. The RLGC line model describes transmission lines as a linear system with distributed parameters (formula 1-2). Losses in conductive materials during signal propagation are described through the surface impedance, which depends on the frequency (formula 3). The dependence $R_s(f) \propto \sqrt{f}$ means that high-frequency components of the signal suffer greater losses than low-frequency components. This leads to an uneven attenuation of the pulse spectrum to a decrease in the amplitude of peak values, blurring of signal edges, and asymmetry in the pulse waveform after passing the transmission line. Such effects are critical in UWB-TL systems, where time distortion directly affects the localisation accuracy or data reception quality. To compensate for them, loss modelling is required at the transmission line design stage.

Any impulse signal x(t) can be represented as a direct Fourier transform (formula 4). According to Fourier's theorem, any limited signal can be represented as a combination of such exponents. Given a known frequency response of the transmission line H(f), the spectrum of the signal after passing through the line is determined by the formula (formula 5): This corresponds to the convolution of the signal with the impulse response of the line in the time domain. The inverse Fourier transform restores the signal in the time domain (formula 6): In applied engineering problems, the analytical Fourier transform is implemented in a discrete form. For this purpose, a discrete Fourier transform is used, which grounds calculations based on a finite number of signal samples (formula 7). This transformation converts the signal from the time domain to the frequency domain, where each X[k] represents the amplitude and phase of the corresponding frequency component. To restore the signal from its spectrum, the inverse Fourier transform is used (formula 8).

The forward and inverse Fourier transform, as well as their discrete implementation, are fundamental tools for

analysing and modelling signals in ultra-wideband transmission lines. These methods were used to accurately describe the change in the spectral structure of the signal during its propagation and calculate the impulse response of the line in terms of real losses and dispersion. Table 2 showed examples of UWB-TL modelling methods used to optimise pulse transmission, minimise losses and preserve signal integrity in high-frequency digital paths and wireless interfaces.

Table 2. *Real-world examples of UWB-TL modelling methods*

Method	Implementation
RLGC model	The RLGC model is used to simulate stripline vertical transitions in high-speed digital interfaces (up to 10 GHz). The R, L, G, C parameters are used to analyse the loss through and dielectric losses, which can be used for optimising transitions to reduce phase distortion and preserve the integrity of picosecond pulses.
Frequency-dependent parameters ($Z_0(f)$, $\alpha(f)$)	They are used for designing mm-wave multilayer UWB filters with a defective ground structure. The simulation addresses frequency-dependent losses in microstrip lines caused by and the dielectric, providing stable signal filtering in the 30-40 GHz range for telecommunications systems.
Phase constant $\beta(f)$	Used to analyse CPS structures in high-speed digital transmission systems. Phase stability modelling compensates for the dispersion that occurs when transmitting picosecond pulses, providing accurate phase balancing for frequencies up to 10 GHz in digital circuits.
Surface resistance Rs(f)	Modelled for MEMS-based coaxial lines in IoT devices. Surface impedance loss analysis enables optimised array design for broadband signal transmission (up to 20 GHz), reducing pulse asymmetry and increasing data transmission efficiency.
Fourier transformation	Used to analyse the spectral and temporal behaviour of UWB signals in wireless networks. The forward and inverse transforms are used to estimate the impulse response, which can be used for predicting signal distortion due to dispersion and losses in real communication channels (up to 15 GHz).

Source: *compiled by the author based on M.-J. Kim et al. (2024), B.-C. Min et al. (2024), Y. Zhu et al. (2024), Y. Weng et al. (2025), P. Poggiolini & Y. Jiang (2025)*

The results of the study confirmed the feasibility of using the RLGC model with consideration of frequency-dependent parameters and the phase constant to analyse the impulse distortion in UWB-TL. This is consistent with a study by Y. Zhang *et al.* (2023), which developed a method for broadband extraction of RLGC parameters for multi-conductor lines using an advanced mode tracking algorithm. The proposed solution ensured high accuracy in determining the frequency-dependent values of resistance, inductance, conductivity, and capacitance (R, L, G, C) in a wide frequency range, which is important for high-frequency modelling.

The evaluation of the influence of frequency-dependent characteristics, such as impedance $Z_0(f)$ and attenuation $\alpha(f)$, on the efficiency of pulse transmission in a high-frequency environment is confirmed by the work of M.-J. Kim *et al*. (2024). The authors implemented an ultra-wideband vertical transition in a coplanar ribbon line for next-generation digital interfaces with an operating range of up to 110 GHz. Although the technical implementation is different from the approaches used in the current study, both approaches emphasise modelling the behaviour of the transmission medium concerning frequency-dependent losses and impedance parameters. In both studies, the line characteristics are matched, which is critical for reducing dispersion-induced phase distortion and ensuring reliable reproduction of the pulse waveform.

K. Mao *et al*. (2022) proposed a new methodology for modelling broadband channels using a continuous frequency response and inverse/direct Fourier transform. As part of this work, the time structure of signals up to 15 GHz was studied, and the characteristic forms of impulse distortion in real conditions were established. The generalised conclusions showed the effectiveness of using frequency analysis to reproduce the dynamics of pulse signals, which corresponded to the results of this study on modelling UWB transmission lines. In the process of modelling UWB transmission lines and antenna structures in the context of WBAN systems, numerical and experimental methods are used. Table 3 provided a comparative overview of common modelling methods, their characteristics, and applications in the field of ultra-wideband technologies.

Table 3. *Methods of modelling UWB transmission lines and their parameters*

Method	Characteristic	Application examples
FDTD	Numerical method for simulating the spatial and temporal evolution of electromagnetic waves in real time. Uses space and time discretisation to solve Maxwell's equations, effective for broadband signals and complex structures.	Modelling of UWB antennas (e.g., Vivaldi) to analyse the propagation of pulsed signals in the range of 3-10 GHz, incorporating dispersion and losses.
FEM	A method for analysing complex geometries and heterogeneous media by breaking down the structure into finite elements. Suitable for modelling UWB structures with irregular shapes,such as metamaterials.	Designing metasurface UWB antennas for WBAN, considering complex metamaterial geometries and dielectric properties for up to 30 GHz.
System identification	Based on experimental impulse or frequency responses to create models of system behaviour. Used to predict signal distortion in real-world conditions	Analysis of the impulse response of UWB wireless network systems to estimate distortions due to dispersion and losses in communication channels (up to 15 GHz).

Source: *compiled by the author based on S.M. Kameli et al. (2024), X. Li et al. (2025), P. Poggiolini & Y. Jiang (2025)*

The FDTD method is effective for modelling the spatial and temporal propagation of signals in complex environments. FEM provides high accuracy when analysing structures with complex geometries, such as metasurface antennas. System identification methods, in turn, describe the behaviour of real systems based on empirical data. The choice of a particular approach depends on the problem formulation, accuracy requirements, and the availability of experimental information. In UWB-TL, the shape of a pulse signal changes due to the nonlinear interaction of its spectral components with the amplitude-phase response of the transmission line. This process can be described as a convolution of the signal spectrum with the frequency response of the transmission line, which leads to distortions in the time waveform. Quantifying such distortions is critical to ensure accurate transmission of short-term pulses in high-bandwidth systems such as wireless networks, IoT devices, or high-speed digital interfaces (Min *et al.*, 2024).

The main parameters that characterise pulse distortion include the time delay of the front and back pulse expansion fronts in the time domain caused by dispersion and frequency-dependent losses α(f). This phenomenon reduces the synchronisation accuracy in UWB systems, which is especially critical for picosecond pulses, the shift of the maximum amplitude of the pulse amplitude peak relative to its initial position due to the uneven phase response β(f) of the transmission line, integral energy loss is the total loss of pulse energy caused by frequency-dependent attenuation (α(f)) due to $R_s(f) \infty \sqrt{f}$ and dielectric losses and dielectric losses. This reduces the signal amplitude, making it difficult to detect. To ensure minimal distortion of pulse signals, it is necessary to optimise the design of the transmission line, its geometry, materials and length. One of the criteria is to limit the length of the transmission line, which should not exceed the critical distortion length, the maximum distance at which dispersion and losses do not lead to significant changes in the pulse shape. This length depends on the frequency range of the signal, the parameters of the RLGC model (R, L, G, C) and the electrophysical properties of the medium. In microstrip lines, the critical length decreases due to dielectric losses, while in coaxial structures, it can be longer due to the stable $Z_0(f)$. One of the problems with UWB-TL is signal loss and associated distortion. To transmit pulses of nanosecond or picosecond duration, the frequency-dependent characteristics of the medium that lead to selective attenuation of spectral components are critical (Table 4).

Table 4. *Types of losses and distortions and their impact on UWB-TL performance*

Influence type	Source	Nature of the impact	Change the signal characteristic	Application examples
Losses	Surface resistance $R_s(f) \infty \sqrt{f}$	Ohmic losses due to skin effect	Attenuation of RF components, reduction of amplitude	Analysis $R_s(f)$ and dielectric losses in microstrip filters for mm-waves (30-40 GHz)
	Dielectric losses tan δ(f)↑	Energy absorption in dielectrics	Reduction of the energy efficiency of the pulse	IoT structures with thin film substrates
	Radiation $\alpha_{rad} \propto f^2$	Energy leakage in unshielded structures	Deterioration of coherence, reduction of power	Microstrip lines
	Impedance heterogeneities $Z_0(f)$	Occurrence of signal reflection $\Gamma \neq 0$	Waveform distortion, multi-path	Stripline transitions up to 10 GHz
Distortion (dispersion)	Frequency variance β(f)	Out-of-sync spectral components	Pulse duration lengthening (), maximum shift	Superconducting Magic-T structures (6-14 GHz)
Distortion (amplitude)	Frequency-dependent attenuation α(f)	Uneven spectrum attenuation	Shape asymmetry, loss of pulse integrity (up to 6 dB per 10 cm)	MEMS arrays for IoT (up to 20 GHz)
Temperature sensitivity	Temperature variation ΔT\Delta TΔT in CPW (co-planar waveguide)	Variations of the phase constant Δβ(f)	Phase instability up to ±10%	CPW structures at $\Delta T = 50°C$
Material sensitivity	Growth of tan δ at $f > 20$ GHz	Increased dielectric losses	Reduced amplitude, increased attenuation	Coaxial arrays for IoT
Impedance sensitivity	Reactive component in $Z_0(f)$ superconductors	Variability of phase velocity	Violation of phase stability, decomposition	Superconducting lines in quantum electronics

Source: *compiled by the author based on M.-J. Kim et al. (2024), B.-C. Min et al. (2024), S. Inoue et al. (2024), Y. Zhu et al. (2024), Y. Weng et al. (2025), X. Li et al. (2025)*

The sources of losses, distortion, and sensitivity to topological parameters of UWB transmission lines indicate the complex nature of pulse signal degradation over a wide frequency range. The ohmic, dielectric, and radiation losses increase with frequency, which necessitates an accurate consideration of $R_s(f)$, tanδ and in the modelling process. Dispersion effects, reflected in β(f) and phase velocity changes, create signal distortion, which is critical for picosecond pulses. In addition, the efficiency of the line depends largely on its topology; coaxial and superconducting configurations have the potential to minimise losses but require special attention to phase stability. When designing UWB systems, it is necessary to apply multi-parameter models capable of reflecting the frequency-dependent behaviour of losses, dispersion and the effect of thermal or geometric fluctuations.

The results obtained in this study on the influence of frequency-dependent losses, dispersion, and phase instability in UWB-TL are confirmed by several studies. V. Monebhurrun *et al*. (2023) considered the fifth generation new radio frequency range 1 UWB antenna as a reference structure for the development of the Recommended Practice for Evaluating the Performance of Consumer Wireless Devices Regarding Human Exposure to Radio Frequency Fields P2816 standard. The emphasis is placed on ensuring stable radiation and phase characteristics, which correlate with the influence of radiation losses $\alpha_{rad} \propto f_2$ identified in this study and the need to control phase shifts during pulse transmission.

Among the approaches to reducing losses in coplanar structures, the implementation of an inverted microstrip transmission line with an integrated EBG filter based on the Gap Waveguide principle, which was studied by L. Inclán-Sánchez (2022), attracts attention. In this structure, the electric field is concentrated in an air gap above a continuous metal layer, which significantly reduces dielectric losses due to reduced interaction with the substrate. In addition, the periodic geometry provides a forbidden band for parasitic modes and at the same time supports broadband transmission with controlled phase characteristics. This confirms the relevance of modelling the losses associated with the dielectric loss tangent tanδ and phase fluctuations in CPW structures analysed in the current study.

The challenges faced in modelling broadband transmission systems include frequency impedance inhomogeneity, phase instability and the need for accurate matching of elements in the high-frequency range. These aspects are discussed in detail in study A. Richter *et al.* (2022), which analyses broadband lines with pronounced inter-element interaction and complex frequency dependence of characteristics. Comparison with the present study confirms the relevance of the chosen methodology for the analysis of distortions caused by variations $Z_0(f)$ and reflections ($\Gamma \neq 0$) in CPW, coaxial and superconducting UWB transmission line configurations. The current study not only supports the existing theoretical approaches but also complements them with practical evaluations in the high-frequency regime. UWB-TLs are used in electronic systems due to their ability to transmit ultra-short pulses with minimal distortion, stable phase characteristics and low losses. Applications include sensor networks, high-speed digital interfaces, millimetre-wave communications (5G/6G), and superconducting and MEMS technologies. Table 5 summarised the areas of UWB-TL application that demonstrate the effectiveness of these structures in the face of increased requirements for signal reliability and accuracy.

Table 5. *Application and technical parameters of UWB-TL in electronic systems*

Application/ technology	Characteristic	Examples of implementation
IoT and WBAN	Metasurface UWB-TLs operating in the pulse transmission mode (UWB-IR, 3-10.6 GHz) provide ultra-short pulses with a duration of 0.1-0.5 ns without distortion. Provide high spatial resolution (<10 cm), which is critical for accurate positioning in medical sensor systems. The structures demonstrate resistance to temperature (up to ±40°C), mechanical (~1 cm), and humidity (ε change <5%) fluctuations, and are easily integrated into flexible wearable devices (LP size <5 mm).	Metasurface UWB antennas for WBAN (3-10 GHz) with >5 dB gain and >7 GHz bandwidth for wireless heart rate/respiration monitoring.
Ultra-fast digital interfaces	UWB-TL in the form of coplanar structures (CPS, CPW) on printed circuit boards is capable of transmitting signals at 25-50 Gbps. Dispersion compensation is achieved due to precise impedance matching (Z_0 = 50±5 Ohm) and geometric optimisation (conductor width ~0.1 mm). Pulse edge preservation is guaranteed by a time distortion of <10 ps.	Phase-balanced CPS structures for digital interfaces (up to 10 GHz) transmitting picosecond pulses with <2 dB loss per 10 cm.
5G/6G systems	UWB-TLs are used as transmission paths in FR2/FR3 systems (24-52 GHz), between TX-ANT, ANT-RX and in filters (BPF, LPF). Provides a bandwidth of >10 GHz, loss <0.5 dB/cm, and low reflection coefficient (Γ<0.1). The design uses striplines or microstrip tracts with materials having a very low loss tangent (tanδ 0.005).	UWB mm-wave filters with a defective ground structure (30-40 GHz) for 5G/6G, with a 12 GHz bandwidth and <1 dB loss.
Superconducting and MEMS technologies	Superconducting UWB-TLs ($R_s \approx 0$ to 100 GHz) provide extremely low losses (<0.01 dB/m) and phase stability (φ<1°), which are critical for quantum sensors and submillimetre systems. MEMS elements enable dynamic change of impedance and phase ($Z_0(f)$, $\beta(f)$) at microsecond rates for adaptive systems.	Superconducting Magic-T structures (6-14 GHz) for mm/submm cameras with <0.1 dB loss; MEMS coaxial arrays for IoT (up to 20 GHz) with tunable bandwidth.

Source: *compiled by the author based on M.-J. Kim et al. (2024), B.-C. Min et al. (2024), Y. Zhu et al. (2024), S. Inoue et al. (2024), Y. Weng et al. (2025), X. Li et al. (2025)*

UWB-TLs have proven to be highly flexible in terms of design and functionality, enabling them to be effectively integrated into a wide range of applications: from medical WBAN systems and ultrafast digital interfaces to 5G/6G components, MEMS and superconducting electronics. UWB-TLs provide high signal transmission characteristics (low loss, phase stability, broadband) that are critical for modern adaptive and sensor systems. At the same time, their effectiveness largely depends on manufacturing accuracy, material stability and operating conditions. UWB-TLs are a priority technology in high-frequency communication systems, provided that geometric and temperature factors affecting the phase and amplitude characteristics of the lines are addressed. Figure 1 illustrated the practical integration of UWB-TL.

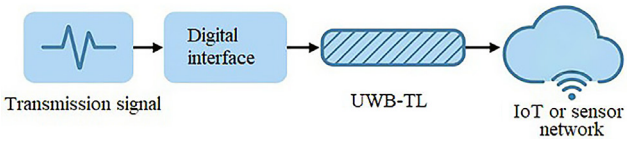

Figure 1. *Block diagram of UWB-TL integration into digital interfaces and sensor networks*
Source: *compiled by the author*

To ensure the effective functioning of UWB-TL in digital systems, it was advisable to formulate several recommendations, the comprehensive implementation of which creates the basis for improving the accuracy, reliability and adaptability of transmission lines. The main factors of influence, including frequency-dependent losses, phase instabilities, and design features of the environment, are addressed. The application of such recommendations helps to reduce signal distortion, improve component matching and ensure high transmission quality even in difficult operating conditions. Table 6 summarised technical approaches that can improve the efficiency of UWB-TL in electronic and sensor platforms.

Table 6. *Engineering and theoretical vectors of UWB-TL improvement*

Recommendation	Description
Extending models for complex environments	Development of analytical and numerical models (FDTD, FEM) to account for inhomogeneities (Δe_r ~ 5-10%), angular rotations (θ ~ 45-90^0), transient elements (ΔZ_0 5-10 Ω) and dispersion ($\beta(f) \propto f$). Integration of the temperature dependence of the surface resistivity ($R_s(f, T) = R_s(f) \cdot [1+\alpha_T (T - T_0)]$) for superconductors (T < 100K) and dielectrics (tanδ (T) 0.001-0.01) in the range of 1-40 GHz.
Modelling nonlinear and adaptive structures	Theoretical justification for MEMS and tunnelled transmission lines with adjustable impedance (ΔZ_0 ~ 5-10 Ω) and phase response ($\Delta\beta(f)$ ~ 0.1 - 0.5 rad/m via control signals (voltage 1-10 V, switching time <1 μs). Nonlinear effects analysis ($\Delta\phi$ ~ 5-20°), (ΔA ~ 0.5 - 2 dB) under dynamic geometry change in real time for IoT and 5G/6G (up to 20 GHz).
Digital distortion compensation	Optimisation of digital inverse filters ($H^{-1}(f)$) based on the impulse response (h(t)) of the transmission line, taking into account frequency-dependent losses ($\alpha(f) \propto \sqrt{f}$, surface impedance ($R_s(f) \propto \sqrt{f}$) and phase dispersion ($\Delta\beta(f)$ ~ 0.01-0.1rad/GHz). Creation of open databases for microstrip, CPS and coaxial LPs (1-40 GHz) for testing AI (Artificial Intelligence)/DSP (Digital Signal Processing) algorithms.
Investigation of UWB lines in the THz band	UWB-TL modelling for 6G front ends (100-1000 GHz), considering micro-/nano-scale effects (λ ~ 0.3-3 mm), reflections (G < 0.05) and interactions with antennas. Analysis of bioengineered media for WBAN (e_r ~ 10-50, tanδ ~ 0.1) and biosensors with picosecond pulses (τ ~ 1 - 10 пс).
Interdisciplinary research	Integration of mathematical physics (solving Maxwell's equations for waveguides), materials science (models e_r, tanδ), superconductors with $R_s(f) \to 0$, computer engineering (DSP, deep learning for h(t) and biomedical engineering (biocompatible dielectrics, WBAN). Orientation to real conditions – temperature fluctuations (ΔT ~ 20 - 70°, humidity up to 80%, (Δe_r ~ 5%)).

Note: *α_T – temperature coefficient of change of surface resistance, reflects the sensitivity of a material to temperature changes, T – current temperature, Kelvin (or °C in case of appropriate conversion), T_0 – usually a fixed reference temperature at which the base temperature is measured $R_s(f)$, THz-range (terahertz frequency range) frequency range from 0.1 to 10 THz (100-10000 GHz), occupying an intermediate position between the microwave and infrared spectra*
Source: *compiled by the author based on B.-C. Min et al. (2024), Y. Zhu et al. (2024), A.M. Elbir et al. (2024), X. Li et al. (2025), S.U. Rehman et al. (2025), Y. Siraj et al. (2025)*

The results of the study showed that one of the areas of development is the adaptation of models to complex real-world conditions considering the terahertz range, temperature dependencies and nonlinear behaviour. S. Iwamatsu *et al.* (2023) demonstrated the prospect of a multiband planar interconnect line capable of efficient operation in the range of 60-340 GHz. The authors focused on reducing reflection and considering geometric inhomogeneities, which correlates with the current study on modelling UWB-TL in the terahertz band for 6G. The data provided by the authors on the response of the system in a microscale waveguide structure is also consistent with the assumptions of the current study on the influence of λ- and Γ-parameters in media with high dielectric contrast.

One of the areas that finds its practical reflection in the scientific literature is the modelling of adaptive UWB structures with the ability to control impedance and phase characteristics. For instance, A. Rajput & B. Mukherjee (2023) demonstrated the implementation of an electronically controlled varicap notch filter capable of changing the characteristic impedance in the range of $\Delta Z_0 \approx 5$ - 10 Ohm and the phase constant $\Delta\beta(f) \approx 0.1$ - 0.5 rad/m in real time. These parameters are confirmed by the engineering vector formulated in the current study, which justifies the need for theoretical modelling of nonlinear effects and controlled signal transmission in adaptive environments. Common to both approaches is the emphasis on switching speed, sensitivity to geometry, and the ability of the structure to maintain transmission stability over a wide frequency range of up to 20 GHz.

This study proposed to address the temperature dependence of the surface resistance $R_s(f, T)$ as one of the factors affecting the phase instability in UWB-TL, for superconducting and dielectric media in the range up to 40 GHz. This approach involved the integration of temperature parameters into dispersion and loss models, which is important for accurate prediction of phase shift and pulse attenuation under conditions of environmental changes. F. Defrance *et al.* (2024) confirmed the validity of this approach: the authors experimentally investigated losses in

amorphous silicon at low temperatures and quantified the behaviour of the dielectric loss tangent tan δ at $T \to 0$ K. The study emphasised the need to consider temperature dependencies in ultrahigh-frequency superconducting systems, which directly supported the position formulated in the current results.

Approaches to digital distortion compensation in transmission lines are actively developing both in the radio frequency and optical ranges. In the study by V. Bajaj *et al.* (2022), devoted to linear and nonlinear distortions in fibre-optic systems, the use of deep neural networks in combination with inverse $H^{-1}(f)$ filters, which provide signal recovery by compensating for amplitude- and phase-dependent losses, proved to be effective. This approach demonstrated the relevance of the method for ultra-wideband environments, where the frequency-dependent parameters $\alpha(f)$, $R_s(f)$ and $\beta(f)$ also cause critical pulse distortion. The digital compensation vector formulated in the current study suggests a similar strategy for constructing a correction filter based on the h(t) characteristic of the medium, considering statistical models of losses and dispersion. This alignment emphasised the versatility of the inverse filtering principle in the tasks of restoring the integrity of a broadband signal. Similar principles of signal optimisation and input data filtering have also proven effective in related fields, particularly in the study by O. Turchyn (2024), where the use of combined neural networks for processing dynamometric signals improved the accuracy of technical diagnostics in complex equipment operating conditions.

Furthermore, the results of the study showed that the adaptation of numerical methods to the conditions of variable dispersion $\beta(f)$, temperature effects on the surface impedance $R_s(f, T)$ and inhomogeneous characteristics of the medium ΔZ_0 can significantly improve the accuracy of modelling pulse transmission in UWB lines. A similar approach was implemented in a study by J. Sarkis *et al.* (2024), where an algorithm was proposed to quickly calculate the spatial power profile in inverse Raman amplification systems, which also addresses frequency-dependent effects and medium inhomogeneities. This solution provided up to 30 times faster computations with high accuracy (<0.05 dBm) and can be adapted to the tasks of modelling UWB structures with complex losses, which was fully consistent with the current study.

Thus, an interdisciplinary approach combining mathematical physics, materials science, computer science, and biomedical engineering ensured realistic modelling and optimisation of UWB-TL in conditions of variable temperature, humidity, and bioelectrical properties of the environment. This approach is important for war-torn Ukraine, as reliable UWB systems can become the basis for restoring critical infrastructure and ensuring stable signal transmission in difficult conditions (communication disruption and power outages). A holistic solution to these challenges will bring the high-frequency signal transmission infrastructure to the level of meeting the challenges of the digital age of the 21st century.

Conclusions

The results of the study showed that UWB-TLs can provide efficient transmission of ultrashort pulse signals with a wide frequency range (over 500 MHz) in telecommunication and sensor systems. It was found that the metamaterial UWB-TLs for WBAN support pulses with a duration of 0.1-0.5 ns without distortion, providing high spatial resolution (<10cm). Coaxial, stripline, microstrip, coplanar (CPS, CPW), and superconducting structures can transmit short pulses, but suffer from distortion due to frequency-dependent losses (surface resistance $R_s(f) \propto \sqrt{f}$, tan δ(f) and dispersion (β(f)), which leads to pulse lengthening and amplitude reduction. The RLGC, FDTD, and FEM models revealed that the geometric inhomogeneities of the transient elements caused phase shifts and multipath reflections that distorted the waveform. It was found that such distortions could be significantly reduced by precise impedance matching and digital compensation in the presence of high-frequency losses. Superconducting lines showed losses of <0.01 dB/m up to 100 GHz, making them effective for quantum and submillimetre systems. The coplanar structures provided data transmission at 25-50 Gbps with time-distortion.

The metamaterial antennas for WBAN provided >5 dB gain and >7 GHz bandwidth, which was essential for accurate positioning in medical systems. The temperature dependence of the surface resistance $R_s(f, T)$ was modelled, which demonstrated the effect of temperature changes on the characteristics of transmission lines. This effect was typical for superconducting and dielectric structures operating in a wide frequency range. Particular attention was also paid to the modelling of variations in the wave impedance (ΔZ_0) and phase constant ($\Delta\beta(f)$), which revealed a significant impact on the pulse transmission parameters. For practical implementation in IoT systems, it is recommended to use MEMS structures with adjustable impedance and phase parameters, for 5G microstrip filters with low losses and wide bandwidth, for WBAN metamaterial UWB antennas with high gain and stable spatial accuracy in the face of environmental fluctuations.

The study was limited to partial consideration of noise and the influence of complex operational factors, such as humidity and micro-/nano-effects in the THz range (100-1,000 GHz). The temperature dependence and material inhomogeneities were partially analysed, but required further improvement to more accurately reproduce real-world conditions. Further research should focus on the development of digital distortion compensation methods using AI and deep learning, as well as the development of temperature-stable materials for UWB systems for use in telecommunications, biosensor technologies, and 6G networks.

Acknowledgements

None.

Funding

None.

Conflict of Interest

None.

References

[1] Bajaj, V., Buchali, F., Chagnon, M., Wahls, S., & Aref, V. (2022). Deep neural network-based digital pre-distortion for high baudrate optical coherent transmission. *Journal of Lightwave Technology*, 40(3), 597-606. doi: 10.1109/JLT.2021.3122161.

[2] Batrakov, D.O., Antyufeyeva, M.S., Batrakova, A.G., & Ruban, V.P. (2024). Ground penetrating radar application for positioning cracks in non-rigid road pavements. In A.K. Nagar, D.S. Jat, D. Mishra & A. Joshi (Eds.), *Intelligent sustainable systems* (pp. 453-464). Singapore: Springer. doi: 10.1007/978-981-99-7569-3_37.

[3] Defrance, F., Beyer, A.D., Shu, S., Sayers, J., & Golwala, S.R. (2024). Characterization of the low electric field and zerotemperature twolevelsystem loss in hydrogenated amorphous silicon. *Physical Review Materials*, 8, article number 035602. doi: 10.1103/PhysRevMaterials.8.035602.

[4] Dubrovka, F.F., Piltyay, S., Movchan, M., & Zakharchuk, I. (2023). Ultrawideband compact lightweight biconical antenna with capability of various polarizations reception for modern UAV applications. *IEEE Transactions on Antennas and Propagation*, 71(4), 2922-2929. doi: 10.1109/TAP.2023.3247145.

[5] Elbir, A.M., Mishra, K.V., Chatzinotas, S., & Bennis, M. (2024). Terahertz-band integrated sensing and communications: Challenges and opportunities. *IEEE Aerospace and Electronic Systems Magazine*, 39(12), 38-49. doi: 10.1109/MAES.2024.3476228.

[6] Fisher, A., Jones, T.R., & Peroulis, D. (2025). Ultra-wideband silicon plasma switches. *IEEE Journal of Microwaves*, 5(3), 677-686. doi: 10.1109/JMW.2025.3559499.

[7] Inclán-Sánchez, L. (2022). Inverted microstrip gap waveguide coplanar EBG filter for antenna applications. *Electronics*, 11(18), article number 2951. doi: 10.3390/electronics11182951.

[8] Inoue, S., Chin, K.W., Uno, S., Kohno, K., Niwa, Y., Naganuma, T., Yamamura, R., Watanabe, K., Takekoshi, T., & Oshima, T. (2024). A design method of an ultra-wideband and easy-to-array magic-T: A 6-14 GHz scaled model for a mm/submm camera. *Journal of Low Temperature Physics*, 216(1-2), 378-385. doi: 10.1007/s10909-024-03150-w.

[9] Iwamatsu, S., Ali, M., Fernández-Estévez, J.L., Tebart, J., Kumar, A., Makhlouf, S., Carpintero, G., & Stöhr, A. (2023). Ultra-wideband multi-octave planar interconnect for multi-band THz communications. *Journal of Infrared, Millimeter, and Terahertz Waves*, 44, 532-550. doi: 10.1007/s10762-023-00926-1.

[10] Kameli, S.M., Refaat, S.S., Abu-Rub, H., Darwish, A., Ghrayeb, A., & Olesz, M. (2024). Ultrawideband Vivaldi antenna with an integrated noise-rejecting parasitic notch filter for online partial discharge detection. *IEEE Transactions on Instrumentation and Measurement*, 73, article number 8001610. doi: 10.1109/TIM.2024.3353284.

[11] Kayalvizhi, A., Sankara Malliga, G., & Seetharaman, R. (2025). Compact inverted E-shaped open-circuited impedance matching stub bandpass filter for wireless applications. *Analog Integrated Circuits and Signal Processing*, 123(1), article number 14. doi: 10.1007/s10470-025-02357-5.

[12] Kim, M.-J., Lee, J.-S., Min, B.-C., Choi, J.-S., Kumar, S., Choi, H.-C., & Kim, K.-W. (2024). Ultra-wideband vertical transition in coplanar stripline for ultra-high-speed digital interfaces. *Sensors*, 24(10), article number 3233. doi: 10.3390/s24103233.

[13] Küpfmüller, K. (1928). On the dynamics of automatic gain controllers. *Electrical Communications Engineering*, 5(11), 459-467.

[14] Lee, G.H., Mohyuddin, W., Kumar, S., Choi, H.C., & Kim, K.W. (2021). Compact wideband coplanar stripline-to-microstrip line transition using a bended structure on a two-layered substrate. *Electronics*, 10(11), article number 1272. doi: 10.3390/electronics10111272.

[15] Li, X., Zhou, Z., Wang, K., Yang, Y., Pang, Z., Zhou, X., Tang, W., Huang, Z., & Lan, D. (2025). UWB metasurface antenna with improved gain and bandwidth for WBAN application. *IEEE Transactions on Consumer Electronics*, 71(2), 5465-5474. doi: 10.1109/TCE.2025.3552597.

[16] Liu, S.-Z., Liu, R., Li, L.-Y., Meng, F.-Y., Xu, S., & Ding, C. (2025). Investigation of miniaturized ultra-wideband circulator based on composite ferrite. *Journal of Physics D: Applied Physics*, 58, article number 205001. doi: 10.1088/1361-6463/adcbb7.

[17] Mao, K., Zhu, Q., Ye, X., Feng, R., Duan, F., Miao, Y., & Song, M. (2022). UWB channel modeling and simulation with continuous frequency response. *China Communications*, 19(11), 88-98. doi: 10.23919/JCC.2022.11.007.

[18] Min, B.-C., Choi, J.-S., Choi, H.-C., & Kim, K.-W. (2024). Ultra-wideband common-mode rejection structure with autonomous phase balancing for ultra-high-speed digital transmission. *Sensors*, 24(19), article number 6180. doi: 10.3390/s24196180.

[19] Monebhurrun, V., Chakrabarti, S., & Quoi, R. (2023). A 5G NR FR1 UWB antenna as benchmark for the development of IEEE standard P2816. In *Proceedings of the 45th annual meeting and symposium of the antenna measurement techniques association* (pp. 1-2). Renton: IEEE. doi: 10.23919/AMTA58553.2023.10293360.

[20] Ogurtsova, T., Blinova, N., Pochanin, G., Nesterenko, M., & Pochanina, I. (2023). Reception of UWB pulsed electromagnetic fields: Ferrite antenna with a two-turns coil. In *Proceedings of the international seminar/workshop on direct and inverse problems of electromagnetic and acoustic wave theory* (pp. 84-89). Tbilisi: IEEE. doi: 10.1109/DIPED59408.2023.10269503.

[21] Oppenheim, A.V., Willsky, A.S., & Nawab, S.H. (1997). *Signals and systems*. Upper Saddle River: Prentice-Hall.
[22] Poggiolini, P., & Jiang, Y. (2025). *Recent advances in real-time models for UWB transmission systems*. doi: 10.48550/arXiv.2504.03873.
[23] Rajput, A., & Mukherjee, B. (2023). Electronically tunable UWB band stop filter using varactor diode. *AEÜ – International Journal of Electronics and Communications*, 164, article number 154610. doi: 10.1016/j.aeue.2023.154610.
[24] Rehman, S.U., Alkanhal, M.A., Ahmad, M., Malik, W.A., Abdulkawi, W.M., Salim, A., & Sheta, A.-F. (2025). Mathematical modeling development and synthesis of tapered transmission line resonators and filters. *Physica Scripta*, 100, article number 015511. doi: 10.1088/1402-4896/ad96e6.
[25] Richter, A., Di Rosa, G., & Koltchanov, I. (2022). Challenges in modeling wideband transmission systems. In J. Leuthold, C. Harder, B. Offrein & H. Limberger (Eds.), *Proceedings of the European conference on optical communication* (article number We1A.1). Basel: Optica Publishing Group.
[26] Roy, S., Mahin, R., & Mahbub, I. (2023). A comparative analysis of UWB phased arrays with combining network for wireless-power-transfer applications. *IEEE Transactions on Antennas and Propagation*, 71(4), 3204-3215. doi: 10.1109/TAP.2023.3243852.
[27] Sarkis, J., Jiang, Y., & Poggiolini, P. (2024). *An algorithm to speed up the spatial power profile calculation in backward Raman amplified systems*. doi: 10.48550/arXiv.2411.12688.
[28] Shi, M., Niu, Z., Yang, H., Xiao, J., Zeng, C., Zhang, Y., Zheng, Z., Hu, W., & Yi, L. (2025). Fast and accurate waveform modeling based on sequence-to-sequence framework for multi-channel and high-rate optical fiber transmission. *Optics Letters*, 50(7), 2286-2289. doi: 10.1364/OL.555880.
[29] Siraj, Y., Khardioui, Y., Alaoui, K.S., & Foshi, J. (2025). High-performance terahertz patch antenna with metamaterials for advanced 6G and biomedical technologies. *Scientific African*, 28, article number e02716. doi: 10.1016/j.sciaf.2025.e02716.
[30] Turchyn, O. (2024). Optimisation of dynamometric data collection and processing to improve the efficiency of neural network diagnostics of a sucker-rod pump. *Bulletin of Cherkasy State Technological University,* 29(3), 55-64. doi: 10.62660/bcstu/3.2024.55.
[31] Weng, Y., Feng, W., Shi, Y., Shen, G., Cao, Y., Tang, Y., Zhu, H., Wu, L.-S., Che, W., & Xue, Q. (2025). Millimeter-wave multilayer ultrawideband common-mode filters using defected ground structure. *IEEE Transactions on Components, Packaging and Manufacturing Technology*, 15(4), 800-809. doi: 10.1109/TCPMT.2024.3517734.
[32] Zhang, Y., Liu, P., Xia, B., Wei, G., Song, Y., & Xu, W. (2023). A new wideband RLGC extraction method for multiconductor transmission lines using improved mode tracking algorithm. *IEEE Transactions on Electromagnetic Compatibility*, 66(1), 293-301. doi: 10.1109/TEMC.2023.3331031.
[33] Zhu, Y., Li, X., & Mao, J. (2024). An ultra-wideband substrate integrated coaxial line array based on silicon-based MEMS process. *Journal of Circuits, Systems and Computers*, 33(18), article number 2550016. doi: 10.1142/S0218126625500161.

Надширокосмугові лінії передачі для цифрових систем нового покоління: моделювання та аналіз

Сергій Бойченко
Аспірант
Харківський національний університет радіоелектроніки
61000, просп. Науки, 14, м. Харків, Україна
https://orcid.org/0009-0008-6118-8314

Анотація. Метою дослідження був теоретичний аналіз моделювання імпульсної передачі у середовищах з надширокою смугою пропускання із врахуванням втрат, дисперсії та фазових зсувів. Використано комплексний підхід, що поєднував математичне моделювання та аналіз електромагнітних процесів у різних топологіях ліній передачі, таких як коаксіальні, стриплайнові, мікросмужкові, а також структури на основі метаматеріалів і надпровідників. Встановлено, що дисперсія, частотозалежні втрати, зумовлені поверхневим опором, який зростав пропорційно кореню частоти, і діелектричними втратами з тангенсом, що залежали від частоти, спричиняли спотворення імпульсів із затримками 10-100 пікосекунд і фазовими зсувами до 20 градусів. Для імпульсів тривалістю 0,5 наносекунди ширина спектру становила близько 2 ГГц, що підтверджувало залежність між тривалістю імпульсу та частотним діапазоном. Моделювання за допомогою телеграфних рівнянь, перетворення Фур'є та чисельних методів, таких як скінченних різниць у часовій області та скінченних елементів, дозволило кількісно оцінити втрати до 3-6 децибел на 10 см і критичну довжину ліній, що залежало від геометричних неоднорідностей. Виявлено переваги надпровідних структур із втратами менше 0,01 децибел на метр до 100 ГГц і копланарних ліній для швидкості передачі 25-50 Гбіт/с. Сформульовано частотно-залежні критерії ефективності, які дозволили обґрунтовано обирати тип лінії залежно від вимог до мінімізації фазових зсувів та затухання імпульсу. Практична значимість результатів полягала в можливості їх використання фахівцями з проєктування телекомунікаційних і сенсорних систем для підвищення надійності та точності передачі даних у реальних умовах експлуатації

Ключові слова: дисперсія; поверхневий опір; імпульсний сигнал; частотозалежні втрати; метаматеріали; надпровідники; фазова стабільність